

Differences in the Time Course of Short-Term Depression Across Receptive Fields Are Correlated With Directional Selectivity in Electrosensory Neurons

Maurice J. Chacron,^{1,2} Natalia Toporikova,¹ and Eric S. Fortune³

¹Department of Physiology, Center for Nonlinear Dynamics, and ²Department of Physics, McGill University, Montreal, Quebec, Canada; and ³Department of Psychological and Brain Sciences, Johns Hopkins University, Baltimore, Maryland

Submitted 22 July 2009; accepted in final form 23 September 2009

Chacron MJ, Toporikova N, Fortune ES. Differences in the time course of short-term depression across receptive fields are correlated with directional selectivity in electrosensory neurons. *J Neurophysiol* 102: 3270–3279, 2009. First published September 30, 2009; doi:10.1152/jn.00645.2009. Directional selectivity, in which neurons respond preferentially to one direction of movement (“preferred”) over the opposite direction (“null”), is a critical computation that is found in the nervous systems of many animals. Here we show the first experimental evidence for a correlation between differences in short-term depression and direction-selective responses to moving objects. As predicted by quantitative models, the observed differences in the time courses of short-term depression at different locations within receptive fields were correlated with measures of direction selectivity in awake, behaving weakly electric fish (*Apteronotus leptorhynchus*). Because short-term depression is ubiquitous in the central nervous systems of vertebrate animals, it may be a common mechanism used for the generation of directional selectivity and other spatiotemporal computations.

INTRODUCTION

Uncovering the mechanisms that are used by neural circuits to perform behaviorally relevant computations is a central goal of neuroscience. One such computation is motion processing, where brain circuits determine the direction of movement of sensory stimuli (Hubel 1959; Hubel and Wiesel 1962). Neurons that exhibit directionally selective responses constitute a form of motion processing unit in the brain: such neurons respond strongly to sensory stimuli moving in a given “preferred” direction but weakly or not at all to the opposite “null” direction. Such responses have been found in a variety of species from flies to primates (Hubel 1959; Hubel and Wiesel 1962; Priebe and Ferster 2005, 2008; Reichardt 1969; Sillito et al. 1981). Directional selectivity has received considerable attention over the past 40 yr and a variety of theoretical models have been proposed and numerous physiological experiments have been conducted to understand the underlying cellular and network mechanisms (Carver et al. 2008; Chance et al. 1998; Priebe and Ferster 2008; Reichardt 1969, 1987). One such mechanism is short-term synaptic depression: mathematical models that include differences in the time courses of short-term synaptic depression across a neuron’s receptive field (RF) can lead to directional responses (Carver et al. 2008; Chance et al. 1998).

Weakly electric fish are well suited for studying directional selectivity. This system benefits from well-characterized neural

circuitry (Carr and Maler 1985; Heiligenberg 1991); the ability to achieve intracellular recordings of CNS neurons in awake, behaving animals (Rose and Fortune 1996); and well-characterized behaviors that require perception of moving sensory images (Cowan and Fortune 2007; Nelson and MacIver 1999). In electrosensory perception, nearby objects produce spatiotemporal distortions of the animal’s self-generated electric field. These electric “images” are sensed by an electroreceptor array on the animal’s skin (Turner et al. 1999). As in the visual system, sensory images are transmitted to the receptor array at the speed of light and there is a direct correlation between object size/position and the image that is detected on the sensor array (Fortune 2006). Information from electroreceptors is transmitted through the hindbrain electrosensory lateral line lobe (ELL) that projects to the midbrain torus semicircularis (TS), a layered structure equivalent to the mammalian inferior colliculus. Previous studies have shown that ELL–TS synapses display short-term synaptic depression (Fortune and Rose 2000). Mathematical modeling studies, however, predict that synaptic depression alone is not sufficient to generate directional selectivity: differences in the time course of short-term synaptic depression across the RF are necessary (Chance et al. 1998).

We examined the contribution of short-term depression to the generation of directional selectivity by stimulating small subregions of TS neuron RFs with stationary stimuli that are known to elicit short-term synaptic depression in these neurons (Fortune and Rose 2000). These stimuli elicited depression with different time courses in both the postsynaptic spiking and membrane potential responses at different locations within the RF. These differences in the time course of depression are strongly correlated with direction selectivity in TS neurons. Further, we used a mathematical model to explore the relations between short-term depression and directional selectivity. The directional selectivity exhibited by the model neuron, which used the spatial measures of short-term depression alone to predict direction selectivity, was significantly correlated with the experimentally measured directional selectivity.

METHODS

Stimulation and recording

Adult specimens (length, 12–18 cm) of the Gymnotiform weakly electric fish, *Apteronotus leptorhynchus*, were used in this study. The surgical and experimental procedures have been described in detail elsewhere (Bastian et al. 2002; Chacron 2006; Chacron and Bastian 2008; Ramcharitar et al. 2006; Rose and Fortune 1996; Toporikova and Chacron 2009) and were approved by the respective institutional animal care and use committees of the Marine Biological Laboratory,

Address for reprint requests and other correspondence: E. S. Fortune, Department of Psychological and Brain Sciences, Johns Hopkins University, 3400 North Charles Street, Baltimore, MD 21218 (E-mail: eric.fortune@jhu.edu).

McGill University, and Johns Hopkins University. Animal husbandry and all experimental procedures followed guidelines established by the Society for Neuroscience and the National Research Council. Fish husbandry and experimental design followed published recommendations (Hitschfeld et al. 2009).

Extracellular recordings from ELL pyramidal cells and TS neurons were made with metal-filled micropipettes (Frank and Becker 1964) as described previously (Bastian et al. 2002; Chacron 2006; Chacron and Bastian 2008; Toporikova and Chacron 2009). Intracellular recordings from TS neurons were made with patch pipettes using previously described techniques (Rose and Fortune 1996). Recordings were made in the first five layers of TS that receive direct input from the ELL (Carr and Maler 1985). Data were acquired with Power1401 hardware and Spike2 software (Cambridge Electronic Design [CED], Cambridge, UK). The majority of recordings were made at the normal resting potential (i.e., no current injection) or less than -0.1 -nA continuous current injection.

Stimuli included moving objects (Ramcharitar et al. 2005, 2006) and electrical signals from both moving and stationary dipoles (Bastian et al. 2002; Chacron 2006; Chacron et al. 2003). The moving object consisted either of a 1.8-cm-wide metal plate with a plastic coating on the side opposite to the animal or of a dipole emitting a constant stimulus (see following text) that was actuated with a pen plotter (HP 7010B) and moved sinusoidally along the fish's rostrocaudal axis over a distance of 20 cm. In both cases, the sinusoid was centered at the animal's midpoint and had a frequency of 0.25 Hz. Therefore the object moved a total of 40 cm over 4 s, corresponding to an average velocity of about 10 cm/s, which is the observed mean velocity of salient sensory images during prey-capture behavior (Nelson and MacIver 1999) and within the velocities of error signals that the fish experience during refuge-tracking behaviors (Cowan and Fortune 2007). These stimuli were repeated ≥ 20 times. We did not observe significant differences in directional selectivity using these two objects (data not shown).

Receptive fields from TS neurons were mapped by using a small dipole identical to the one used previously for ELL pyramidal cells (Bastian et al. 2002). The dipole was placed near the side of the animal (within 1 mm of the skin) at various rostrocaudal positions at the level of the midline and responses were accumulated at these positions. We used 4-Hz sinusoidal amplitude modulations (AMs) to map RFs, as done previously for ELL pyramidal cells (Bastian et al. 2002). This temporal frequency is also close to the principal temporal frequency component of movement during prey-capture experiments (Nelson and MacIver 1999) and the obtained maps should therefore be useful in predicting directional selectivity to moving objects mimicking this behaviorally relevant situation.

We also used 20-Hz bursts to map RFs of TS neurons. These stimuli consisted of five cycles of a 20-Hz sine wave (250-ms duration) followed by 750 ms of silence, repeated 300 times for extracellular recordings and at least six times for intracellular recordings. These stimuli are known to elicit short-term depression at ELL-TS synapses when presented via global stimulation geometry to the entire animal (Fortune and Rose 2000).

Stationary, localized stimuli were sinusoidal or constant AMs of the animal's own electric organ discharge (EOD) that were generated by multiplying EOD mimic waveforms with sinusoidal signals. The EOD mimic consisted of a train of single sinusoids of a duration slightly less than that of a single EOD cycle synchronized to the zero crossings of the animal's own EOD. "Contrasts" (depth of the AM) were similar to those used in previous studies (~ 10 – 20%) (Bastian et al. 2002; Chacron and Bastian 2008; Chacron et al. 2005). The resulting signal was presented to the animal via the local dipole, as done in previous experiments (Bastian et al. 2002) using a custom-made linear stimulus isolation unit (Fortune Laboratory Industries, Baltimore, MD).

Data analysis

Data analysis was performed using Spike2 (CED), Origin (Origin-Labs, Northampton, MA), and custom-made routines in Matlab (The MathWorks, Natick, MA). Intracellularly recorded membrane potentials were either low-pass filtered (40 Hz, finite impulse response [FIR] filter in Spike2) to remove the sodium action potentials or band-pass filtered (100–800 Hz, FIR filter in Spike2) to select the action potentials. Spiking responses were accumulated as peristimulus time histograms (PSTHs) and low-pass-filtered membrane potentials were accumulated as average membrane potential waveforms during stimulus trials. The directional selectivity index (DSI) was computed as

$$DSI = \frac{R_{HT} - R_{TH}}{\max(R_{HT}, R_{TH})} \quad (1)$$

where R_{HT} and R_{TH} are the responses to the moving object in the head-to-tail and tail-to-head directions, respectively. DSI ranges from -1 (the neuron responds only when the object moves in the tail-to-head direction) to 0 (the neuron responds equally to either direction) to 1 (the neuron responds only when the object moves in the head-to-tail direction). We quantified spiking responses as the peak firing rate in the PSTH in each direction. We quantified the subthreshold membrane potential response with action potentials removed as the difference between the maximum and baseline values in each direction (spikes removed).

To determine possible errors in the DSI values obtained from our data, we ran simulations in a model that displays no directional selectivity: the rate-dependent Poisson process, where the rate is given by (in Hz): $r(t) = 20 + \{40 \times \exp[-(t - 0.5)^2/0.1]\}$, where $t \in [0, 1]$. We chose a baseline rate of 20 Hz since it corresponds to the mean firing rate observed in our data sample. Here the time t is expressed in seconds. This process was simulated numerically (in Matlab) 300 times, with binwidth $t_{bin} = 1$ ms. Briefly, the content of each bin was set to zero and we generated a uniformly distributed random number between 0 and 1 for each bin: if that random number was less than the probability of obtaining a spike in this bin $P = 20 \times 0.001$, then a spike occurred in that bin. We set the value of bin i to $1/t_{bin}$ if a spike occurred in that bin and 0 otherwise. We pooled the first 150 trials and computed the PSTH from these binary sequences; similarly, we pooled the last 150 trials and computed the PSTH from those binary sequences as well. We assumed that the former PSTH represents the response in the head-to-tail direction and the latter, the response in the tail-to-head direction, and computed the DSI as described earlier; we repeated this procedure 1,000 times. Although in theory the DSI should be zero for this process, our numerical values were normally distributed around zero with mean -0.014 ± 0.019 and SD of 0.254 ± 0.038 . If we instead looked at the distribution of the absolute value of DSI, we found that this distribution had a nonzero mean of 0.0936 ± 0.0714 , whereas, in theory, we should obtain $|DSI| = 0$. We therefore corrected for this bias when testing whether distributions of $|DSI|$ obtained from TS and ELL neurons were significantly different from zero. This was done by comparing each group of $|DSI|$ values to a surrogate sequence of $|DSI|$ values with the same length generated by the Poisson process using a Wilcoxon rank-sum test.

We quantified the peak response R_1 , during the first stimulation cycle of a 250-ms-long 20-Hz sine wave, as either the peak firing rate for extracellular data or peak PSP amplitude for intracellular data. The peak response R_5 was computed in the same fashion during the last cycle of the stimulus. The time constant τ was obtained by fitting the function $b + a \exp[-(t - t_0)/\tau]$ to the data $[t_i, R_i]_{i=1,5}$, where t_i is the time at which R_i occurs; this was performed using the nonlinear least-squares fitting tool in Origin (OriginLabs). We identified the greatest and smallest τ values across different positions and computed the difference (rostral-caudal) as a function of DSI.

Responses to sinusoidal stimulation delivered by a dipole located at different rostrocaudal positions were accumulated as phase histo-

grams that were used to compute the gain g and phase ϕ of the response at that position by fitting the function $R(t) = g \sin(2\pi ft + \phi)$ to the phase histogram. We take $-\pi < \phi \leq \pi$, with $\phi = 0$ corresponding to a local maximum of the sinusoid (Bastian et al. 2002).

We built X–T plots as described previously (Adelson and Bergen 1985) using either the responses to continuous 4-Hz sinusoidal stimulation or to 20-Hz bursts accumulated at different rostrocaudal positions. These positions were converted to a spatial phase, with phase 0 being at the tip of the animal's rostrum. For each neuron, we normalized the response to either of the largest values of gain g across rostrocaudal positions for sinusoidal stimuli. X–T plots for depression were generated in the following manner: the responses obtained to stationary “burst” stimuli at different positions were accumulated as PSTHs and fitted with an exponential decay. These fitted responses were normalized using the maximum response value and plotted as a function of time and position.

We computed Pearson's correlation coefficient R and tested for statistically significantly different values from 0 using standard techniques covered in statistics textbooks (Newbold 2006). Briefly, the t -value is obtained from the correlation coefficient R and the sample size N by

$$t = \frac{R}{\sqrt{(1 - R^2)/(N - 2)}} \quad (2)$$

from which one can perform a t -test to test for the hypothesis that the correlation coefficient is null.

Modeling

We built a mathematical model of a given TS neuron's RF. This was achieved by discretizing the animal's rostrocaudal axis into bins of length $d = 5$ mm. We always took $x = 0$ to be at the tip of the animal's rostrum. For the model in which stationary sinusoidal stimuli were used, the response $r_i(t)$ of bin i was given by $G_i = g_i[\Theta(t - t_i) \text{ sign}(\varphi_i)]$ when the object is inside bin i and 0 otherwise, where g_i and $-\pi < \varphi_i \leq \pi$ are, respectively, the gain and phase obtained experimentally from sinusoidal stimulation. For the model with synaptic depression, the response $r_i(t)$ of bin i was given by $G_i = \Theta(t - t_i)g_i \exp(-t/\tau_i)$, where τ_i is the depression time constant obtained from experimental data, when the object is inside bin i and 0 otherwise. Here $\Theta(\dots)$ is the Heaviside function [$\Theta(x) = 1$ if $x \geq 0$ and $\Theta(x) = 0$ otherwise] and t_i is the time at which the object moving at a speed of 10 cm/s first enters bin i .

In both cases, the TS neuron was modeled as a passive leaky integrator

$$C \frac{dV}{dt} = -g_{\text{leak}}(V - E_{\text{leak}}) + A \sum_{i=1}^N R_i(t) + I \quad (3)$$

We used a Euler algorithm to numerically simulate the model with $dt = 0.0025$ ms. Other parameter values used were $g_{\text{leak}} = 0.18 \mu\text{S}$, $E_{\text{leak}} = -70$ mV, $C = 1$ nF, $A = 1$ nA, and $I = -1.1$ nA.

RESULTS

TS neurons exhibit directional selectivity

We recorded the responses of 49 TS neurons in vivo to moving objects (Fig. 1). A moving bar stimulus was moved sinusoidally back and forth along the rostrocaudal axis of the animal (Fig. 1A). Most TS neurons in our data set had directionally biased responses to this stimulus: the peak response was greater in one direction, termed “preferred,” than the opposite direction, termed “null” (Fig. 1B). We

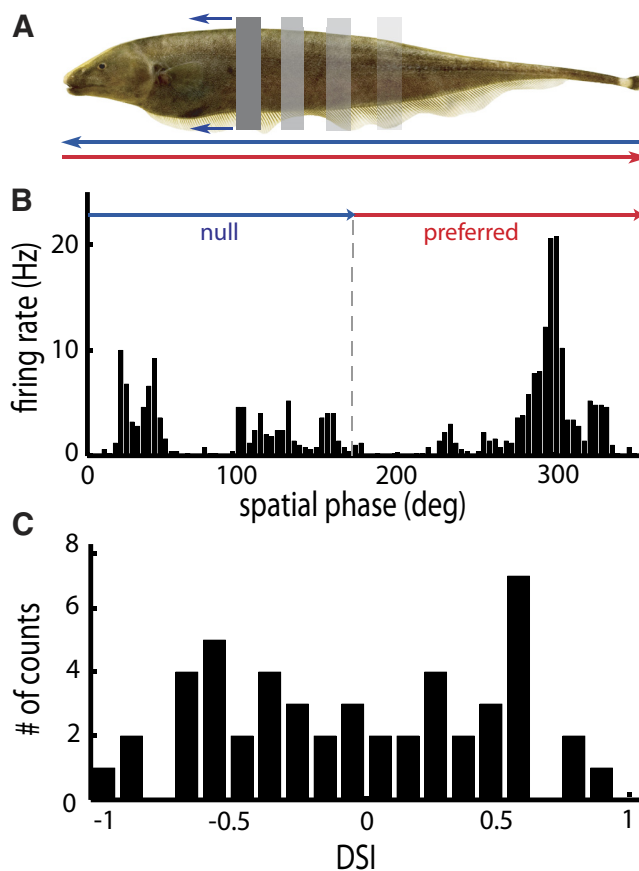


FIG. 1. Torus semicircularis (TS) neurons display directional selectivity. *A*: schematic of the moving object stimulus. A metal bar with plastic backing was moved back and forth along the side of the animal's body. Black indicates tail-to-head movement and gray, head-to-tail. *B*: peristimulus time histogram (PSTH) of a TS neuron to the moving object. This neuron displays a greater peak firing rate when the object moved in the head-to-tail direction (preferred) as opposed to the tail-to-head direction (null). *C*: distribution of directional selectivity index (DSI) values for our data sample. The distribution did not have a mean that is significantly different from zero ($P = 0.1149$, sign-test, $n = 49$), but did display peaks at around -0.6 and 0.6 .

quantified this bias using the DSI, which ranges between -1 (the neuron responds only when the object moves in the tail-to-head direction) to 1 (the neuron responds only when the object moves in the head-to-tail direction). The distribution of DSI values obtained from our data were symmetric around 0 and displayed peaks near -0.6 and 0.6 (Fig. 1C), indicating that roughly 50% of neurons preferred the tail-to-head direction and the other 50% preferred the head-to-tail direction.

ELL neurons that project to TS do not exhibit directional selectivity

The simplest explanation for the directionally biased responses in TS is that they are inherited from the activity of afferent neurons. In weakly electric fish, electroreceptors on the skin surface respond to electrosensory stimuli and relay this information to pyramidal cells within the electrosensory lateral line lobe (ELL) (Maler 1979; Maler et al. 1981, 1991) (Fig. 2A): pyramidal cells are the sole source of ascending electrosensory

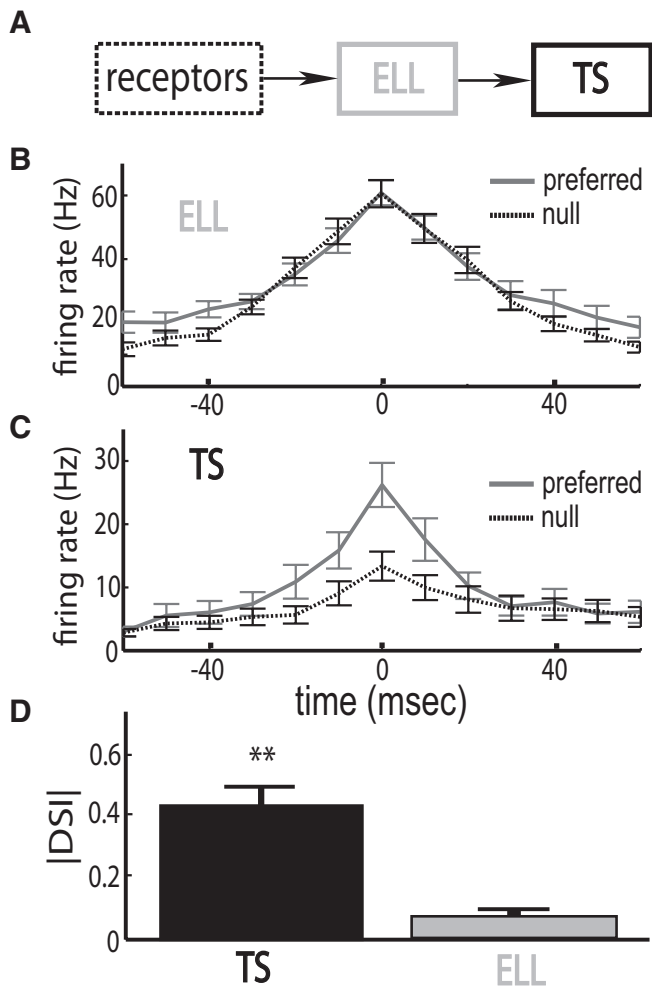


FIG. 2. Directional selectivity emerges at the level of the TS. *A*: primary electrosensory receptor afferents converge onto electrosensory lateral line lobe (ELL) neurons, which in turn project onto TS neurons. *B*: population-averaged responses in the preferred and null directions were roughly equal for ELL neurons. *C*: population-averaged responses displayed a greater maximum in the preferred direction for TS neurons. *D*: population-averaged $|DSI|$ values were significantly different from zero for TS neurons but not for ELL neurons (see text for details).

input to TS. We recorded pyramidal cell responses to the same moving object stimulus. Responses to the preferred and null directions were similar in ELL neurons, indicating a lack of direction selectivity (Fig. 2*B*). In contrast, TS neurons typically showed differences in the responses to the two directions of movement (Fig. 2*C*). We looked at the distributions of the absolute directional bias in both ELL and TS neurons and tested whether their means were statistically significantly different from 0. The average absolute directional bias in ELL ($|DSI| = 0.1041 \pm 0.0108$) (Fig. 2*D*) was not significantly different from zero ($P = 0.1791$, Wilcoxon rank-sum test, $n = 38$), indicating that ELL neurons are not directionally selective and confirming previous results (Bastian 1981). In contrast, the absolute directional bias in TS ($|DSI| = 0.4213 \pm 0.0583$) was significantly greater than zero ($P < 10^{-3}$, Wilcoxon rank-sum test, $n = 23$). These results show that the ELL is not the source of directionally biased responses in TS.

Directional selectivity to moving objects in TS is not correlated with center-surround receptive field properties

We mapped the RFs of TS neurons using a small non-moving dipole that was placed at different locations along the side of the animal (Bastian et al. 2002) (Fig. 3*A*). TS neurons often displayed large RFs with center-surround organization. Interestingly, we found neurons that displayed identical responses to these stationary, spatially localized stimuli that were largely independent of location along the side of the animal (Fig. 3*B*). We used X-T plots (Adelson and Bergen 1985; Priebe and Ferster 2008) to characterize the RF properties of TS neurons. The X-T plot from the same neuron as that in Fig. 3 shows a response that is largely independent of position (Fig. 4*A*). Consequently, one would predict that this neuron would show weak or no directional selectivity. Another example neuron displayed a response to stationary stimuli that were strongly dependent on the dipole's position (Fig. 4*B*); inspection of this map would suggest that this neuron should display a greater response when the object moves from left to right than vice versa.

Responses of these two neurons to the same dipole used as a moving stimulus are shown in Fig. 4, *C* and *D*, respectively. The first example neuron showed a strong directional bias, whereas the second example neuron showed no directional bias, which is opposite to what was predicted from the RF maps. Although these two examples do not support a role of the center-surround organization of excitation and inhibition in the generation of direction selectivity, there may nevertheless

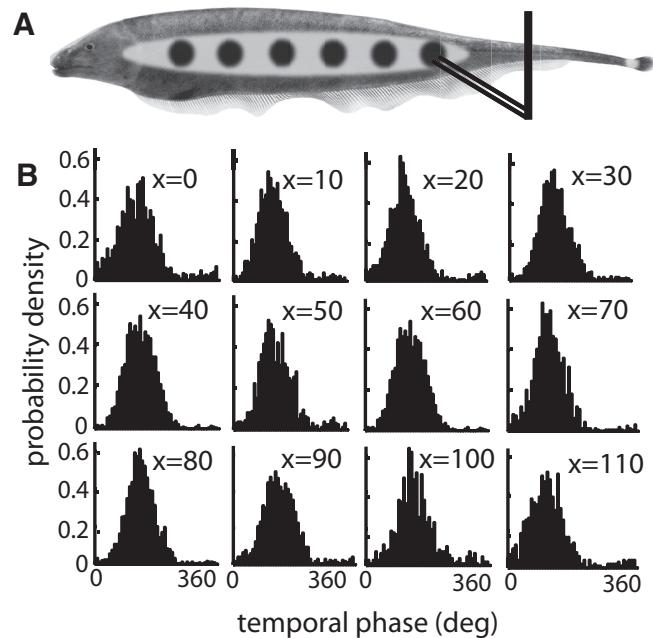


FIG. 3. Mapping the receptive field properties of TS neurons. *A*: schematic of the experimental setup: a small dipole (black lines) is positioned at different rostrocaudal positions (black dots) throughout the receptive field of the TS neuron (gray area). *B*: responses to 4-Hz sinusoidal stimulation were accumulated at each position (in mm) and are shown as cycle histograms: these were used to compute the gain G_i and phase ϕ_i at that position. Responses of this particular neuron to sinusoidal stimulation were largely independent of the dipole's position.

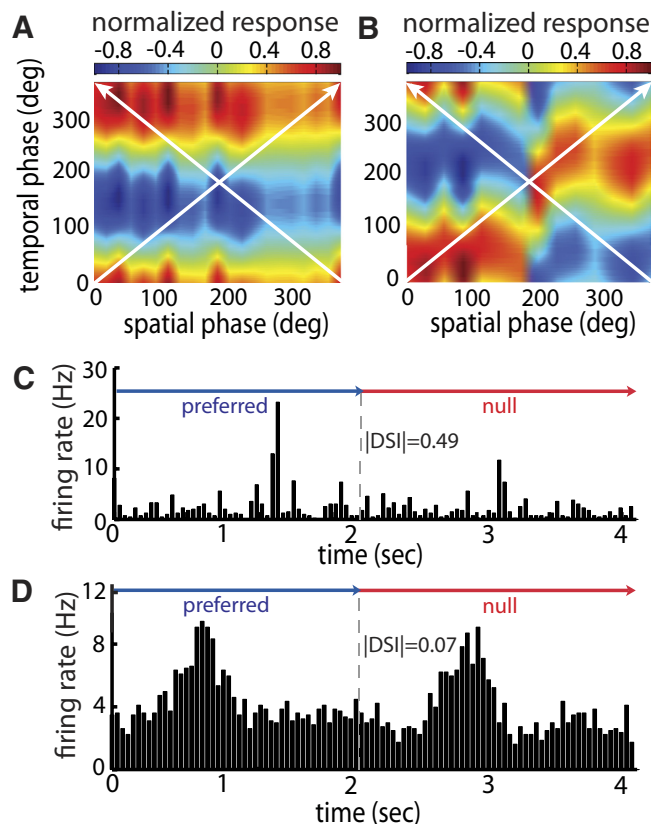


FIG. 4. Center-surround organization does not predict directional selectivity in TS neurons. *A*: receptive field (RF) map from the same neuron as in Fig. 3 showing a response that is largely independent of position within the receptive field. One would predict weak directional selectivity from this map, as can be seen by comparing the responses to moving stimuli in both directions as represented by the white arrows. *B*: RF map from another example neuron that showed a strong center-surround receptive field organization. In contrast, one would predict strong directional preference going from spatial phase 0 to spatial phase 360° (i.e., head-to-tail motion) for this neuron by comparing the responses to moving stimuli in both directions as represented by the white arrows. *C*: response of the same neuron as in *A* to the dipole moving: this neuron showed significant directional selectivity that does not fit the prediction from the RF map. *D*: response of the same neuron as in *B* to the dipole moving: in contrast, this neuron showed no significant directional selectivity, which again does not fit the prediction from the RF map.

be a correlation between direction selectivity and the center-surround organization when we look across our data set. To address this issue, we then built a mathematical model that incorporated the experimentally measured responses to stationary sinusoidal stimuli at different rostrocaudal positions for a given neuron (see METHODS). We used this model to predict the DSI and compared it to the experimentally measured value for that neuron. We found no significant correlation between both quantities ($R = 0.3131$, $P = 0.1363$, $n = 24$) across our data. These results strongly argue against the contribution of the center-surround RF properties to direction selectivity in TS neurons for moving stimuli whose velocities are close to those found in behaviorally relevant prey-capture (MacIver et al. 2001; Nelson and MacIver 1999) and refuge-tracking situations (Cowan and Fortune 2007). We note, however, that they do not preclude a putative involvement of center-surround characteristics in directional responses to objects moving at higher velocities.

Differences in the time constants of depression within the receptive field are correlated with directional selectivity

Previous modeling studies have shown that directional selectivity can be generated by differential temporal filtering of inputs from different zones within the neuron's RF (Borst 2007; Borst and Egelhaaf 1989; Carver et al. 2008; Chance et al. 1998; Reichardt 1969). Two modeling studies suggest that short-term synaptic depression can be a potential source of differential temporal filtering of inputs (Carver et al. 2008; Chance et al. 1998). The mechanism by which different time constants of depression across the RF can give rise to directional selectivity is summarized in Fig. 5. In the simplest form, the model consists of two inputs from two spatially distinct zones within the RF that are associated with different time constants of depression: the resulting postsynaptic potential (PSP) from stimulating the left zone decays with a shorter time constant than the PSP resulting from stimulating the right zone (Fig. 5A). When stimulated with a moving object, this model gives rise to an output that depends on the direction of motion:

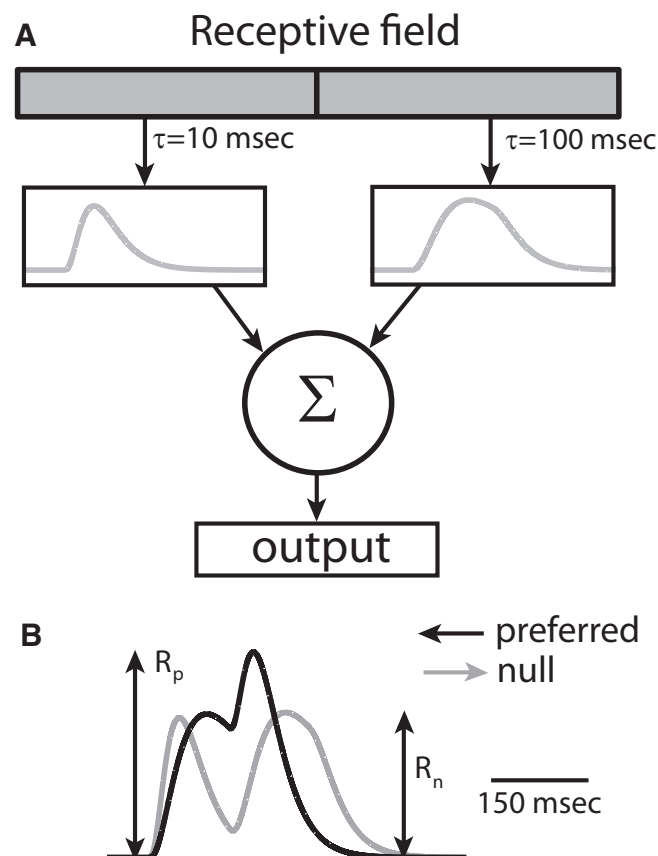


FIG. 5. Summary of the mechanism by which different time constants of depression can give rise to directional selectivity. *A*: model diagram in the case where inputs from 2 spatially distinct zones within the receptive field are differentially processed with 2 different time constants of depression and give rise to postsynaptic potentials (PSPs) with different temporal profiles. Stimulating the left zone gives rise to a PSP that decays with a fast time constant (10 ms), whereas stimulating the right zones gives rise to a PSP that decays with a slow time constant (100 ms). The model's output is taken to be the sum of these 2 inputs. *B*: model output when an object moves from right to left (black) and from left to right (gray) across the receptive field. The height of the compound PSP is given by R_p and R_n when the object moves from right to left and from left to right, respectively.

movement from right to left gives rise to a compound PSP whose maximum value is greater than that when the object moves from left to right (Fig. 5B). This can be explained as follows: when the object moves from left to right, the fast PSP is elicited first and the slow PSP last, leading to very little overlap and little summation. In contrast, when the object moves from right to left, the slow PSP is elicited first and the fast PSP last, leading to greater overlap in time and thus greater summation, which leads to a greater maximum value (Carver et al. 2008; Chance et al. 1998).

To experimentally test the hypothesis that differences in short-term depression across a receptive field can contribute to the generation of direction selectivity, we again stimulated small subregions within a given neuron's RF (Fig. 6A), with stationary, spatially localized electrosensory signals. In this experiment, the signals were transient 20-Hz oscillations,

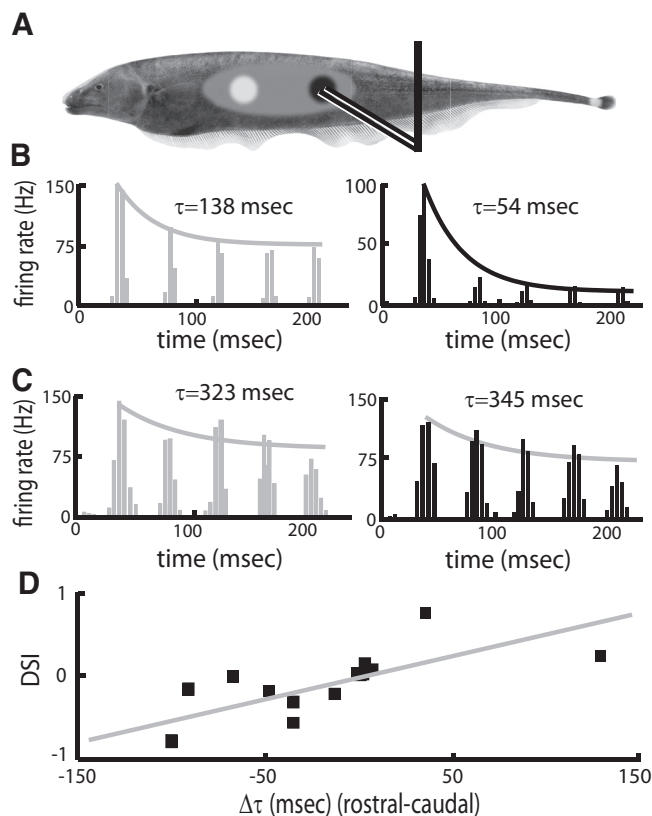


FIG. 6. Directionally selective TS neurons display variations in their short-term depression to stationary stimuli delivered at different spatial locations within the receptive field. *A*: a spatially localized stimulus is delivered via a dipole (black lines) that stimulates small regions (black and light gray dots) within the receptive field (dark gray area) of a TS neuron. The 2 example stimuli, delivered at 2 different locations, are shown in red and blue. *B*: response of a directionally selective TS neuron to a stationary 20-Hz sinusoidal stimulus delivered rostrally at the gray position (*left*) and black positions (*right*) with best exponential fits. Note that the response at the black position shows more pronounced decay and thus gives rise to a lower decay time constant. *C*: response of a nondirectionally selective TS neuron to the same sinusoidal stimulus at the red position (*left*) and the blue position (*right*). Note that both responses have similar time courses and thus similar time constants of decay. *D*: the directional bias was strongly correlated with the difference in decay time constants measured from stationary stimuli across different rostrocaudal positions ($R = 0.77$, $n = 15$, $P < 10^{-3}$).

which are known to elicit short-term synaptic depression from midbrain neurons (Fortune and Rose 2000).

Strongly directionally selective neurons typically displayed slowly decaying peak responses at one end and rapidly decaying responses at the other end of their RF (Fig. 6B). We quantified this depression in the responses by fitting an exponential to the peak response during each stimulus cycle (see METHODS). The resulting depression time constants were then superimposed with the responses (Fig. 6B). In contrast, nondirectionally selective neurons did not show differences in the depression time constants at different locations in the RF and tended to show slower depression time constants (Fig. 6C). In fact, we found a strongly significant negative correlation between $|DSI|$ and the fastest depression time constant measured across the RF for our data ($R = -0.78$, $P \ll 10^{-3}$, $n = 18$). We next explored the relationship between directional selectivity and differences in depression time constants across the RF: we found a strong positive correlation between DSI and the greatest difference in depression time constants across the RFs (Fig. 6D; $R = 0.77$, $n = 18$, $P < 10^{-3}$).

To further examine the relationships between the spatial arrangement of short-term depression within the RF and direction selectivity, we computed X-T plots using the experimentally measured depression time constants at several different locations within the RF of a TS neuron. These were obtained by plotting the exponential fit as a function of time and position. An example X-T plot from a neuron that displayed slow/fast depression in the rostral/caudal parts of its RF shows a strong asymmetry that would suggest that this neuron was directionally selective for movement from spatial phase 0 to spatial phase 360° (i.e., head-to-tail direction; Fig. 7A). This neuron did indeed show a strong directional bias in the head-to-tail direction with $DSI = 0.667$. In contrast, an X-T plot from a neuron that displayed fast depression at its RF edges separated by slower depression near the middle shows relative symmetry in the X-T plot, suggesting weaker direction selectivity (Fig. 7B). This neuron showed much weaker directional selectivity with $DSI = 0.13$.

To quantitatively assess whether the differences in depression time constants measured across the RF could predict the directional responses of TS neurons, we built a mathematical model that consisted of passive integration of convergent inputs from across the RF (Fig. 7C). We performed numerical simulations using this passive model, with the depression time constants obtained experimentally. The role of the differences in short-term depression in generating direction selectivity was supported by a strongly significant correlation between the predicted directional bias from the model and experimentally obtained measures ($R = 0.88$, $n = 18$, $P < 10^{-3}$).

Sources of depression and direction selectivity: comparisons of extracellular spiking activity and intracellular PSPs

What is the source of depression in the spiking response? To answer this question, we performed intracellular recordings from TS neurons and compared their spiking and subthreshold membrane potential responses to stationary stimuli. These recordings revealed that the depression in the spiking response to stationary local stimuli was largely due to depression of the underlying PSP amplitude: more or less pronounced depression in the spiking response was accompanied by more or less

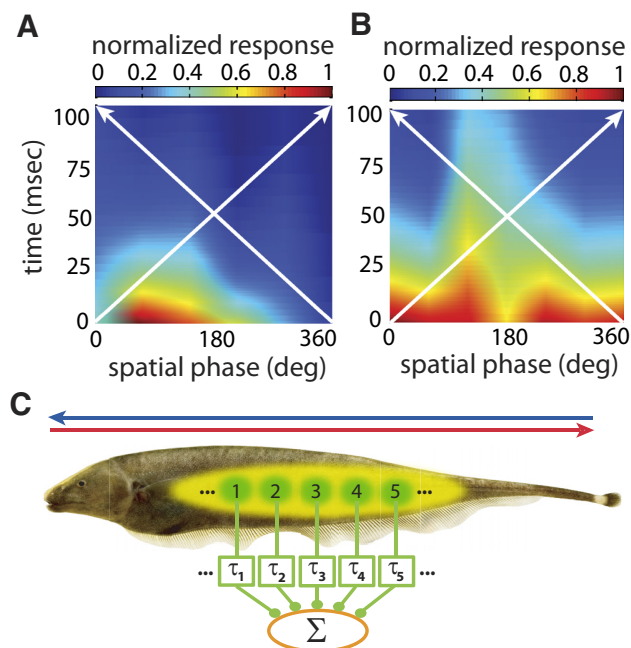


FIG. 7. Differences in time constants of depression across the receptive field correlate with the observed directional bias. *A*: example X–T map of depression across the receptive field from a strongly directionally selective neuron. This map was obtained by plotting the exponential fits obtained at different rostrocaudal positions as a function of time (y-axis) and position (x-axis). The directional selectivity can be assessed by comparing the responses to moving stimuli in both directions as represented by the white arrows. *B*: example X–T map from a weakly directionally selective neuron. The directional selectivity can again be assessed by comparing the responses to moving stimuli in both directions as represented by the white arrows. *C*: schematic of a model for the generation of direction selectivity using depression time constants measured across rostrocaudal positions along the animal. Yellow represents a receptive field in which 5 measurements of the time constant of depression were made (green dots, τ_1 – τ_5). In the model, we sequentially stimulated the subregions of the receptive field in both directions (red and blue arrows). This information was transmitted to a postsynaptic neuron through model synapses. The short-term depression at these synapses matched experimentally obtained measures. The direction selectivity of a summing postsynaptic neuron (orange) was measured.

pronounced depression in the subthreshold membrane potential response (Fig. 8, *A* and *B*). As previously described (Rose and Fortune 1999), the amplitudes of PSPs elicited by these depressing stimuli typically varied from cycle to cycle and, in most neurons, showed a weak oscillation.

We quantified the decay in the PSP amplitude by fitting an exponential function to the peaks of the response (see METHODS). We observed a strong correlation between the depression time constants obtained from the membrane potential and spiking responses (Fig. 8*C*, $R = 0.81$, $P < 10^{-3}$, $n = 13$). Furthermore, the data were not significantly different from the identity line ($P = 0.80$, Wilcoxon rank-sum test, $n = 13$), indicating that depression seen in the spiking activity is due to depression of PSP amplitudes. The time constants appear to form two clusters: a fast cluster around 10 ms and a longer cluster with values in the hundreds of milliseconds. In vitro recordings will be necessary to investigate the mechanisms underlying these differences, which may have important functional consequences (see DISCUSSION).

In the same light, we also quantified the directional bias in the membrane potential, comparing it with the directional bias

in the spiking response to moving objects (Fig. 8*D*), and found a strong positive correlation between both quantities ($R = 0.99$, $n = 18$, $P \ll 10^{-3}$) that was not significantly different from the identity line (Fig. 8*E*, $P = 0.38$, Wilcoxon rank-sum test, $n = 18$). These data show that the membrane potential response already contains all the directional information and further supports that differences in the short-term depression time constants across the RF of TS neurons mediate their directionally biased responses, justifying the use of a linear integrator for the mathematical model.

Source of short-term depression in TS

What are the mechanisms underlying the observed differences in short-term depression time constants in TS? One possibility is that these differences originate in the presynaptic patterns of action potentials of ELL neurons: input from different subregions within the RF could come from ELL neurons with different adaptation in their spiking responses. The ELL is composed of three parallel maps of the body surface that all project to TS (Carr and Maler 1985; Krahe et al. 2008; Shumway 1989a,b). A recent study of the differential temporal filtering properties of ELL neurons in all three maps has revealed adaptation time constants within the ranges of depression time constants observed in TS neurons (Krahe et al. 2008): neurons within the centromedial segment (CMS) had the longest (>200 ms) adaptation time constants, whereas neurons within the lateral segment (LS) had the shortest (<20 ms) adaptation time constants.

Since strongly directionally selective TS neurons had both short and long depression time constants, this would imply that they should receive input from both the CMS and LS maps of the ELL. However, because weakly directionally selective TS neurons had longer depression time constants on average, they should then preferentially receive inputs from the CMS map. Activity in these ELL maps also differ in another overt way: LS neurons display strong phase locking to the EOD, whereas CLS and CMS neurons do not (Krahe et al. 2008).

We therefore quantified the degree of phase locking to the EOD to examine the contributions of the maps to the responses of individual TS neurons. Although some neurons displayed strong phase locking to the EOD, suggesting that they receive input from LS, these neurons tended to have the least directional selectivity. Indeed, there was a significant negative correlation between phase locking to the EOD and directional selectivity ($R = -0.57$, $P = 0.0045$, $n = 23$), indicating that neurons that showed the most directional selectivity tended to show the least phase locking to the EOD. These results speak against a possible contribution of the computational features found across ELL maps for the generation of directional selectivity in TS. Nevertheless, because we do not know the relative distribution of depressing and nondepressing efferent synapses from particular maps and/or classes of ELL neurons, we currently cannot assess particular hypothetical functional organizations of inputs to TS neurons. Future experiments, including direct stimulation of individual ELL maps and in vitro studies, will be necessary to assess the relative contributions and functional organization of ELL efferents to the TS.

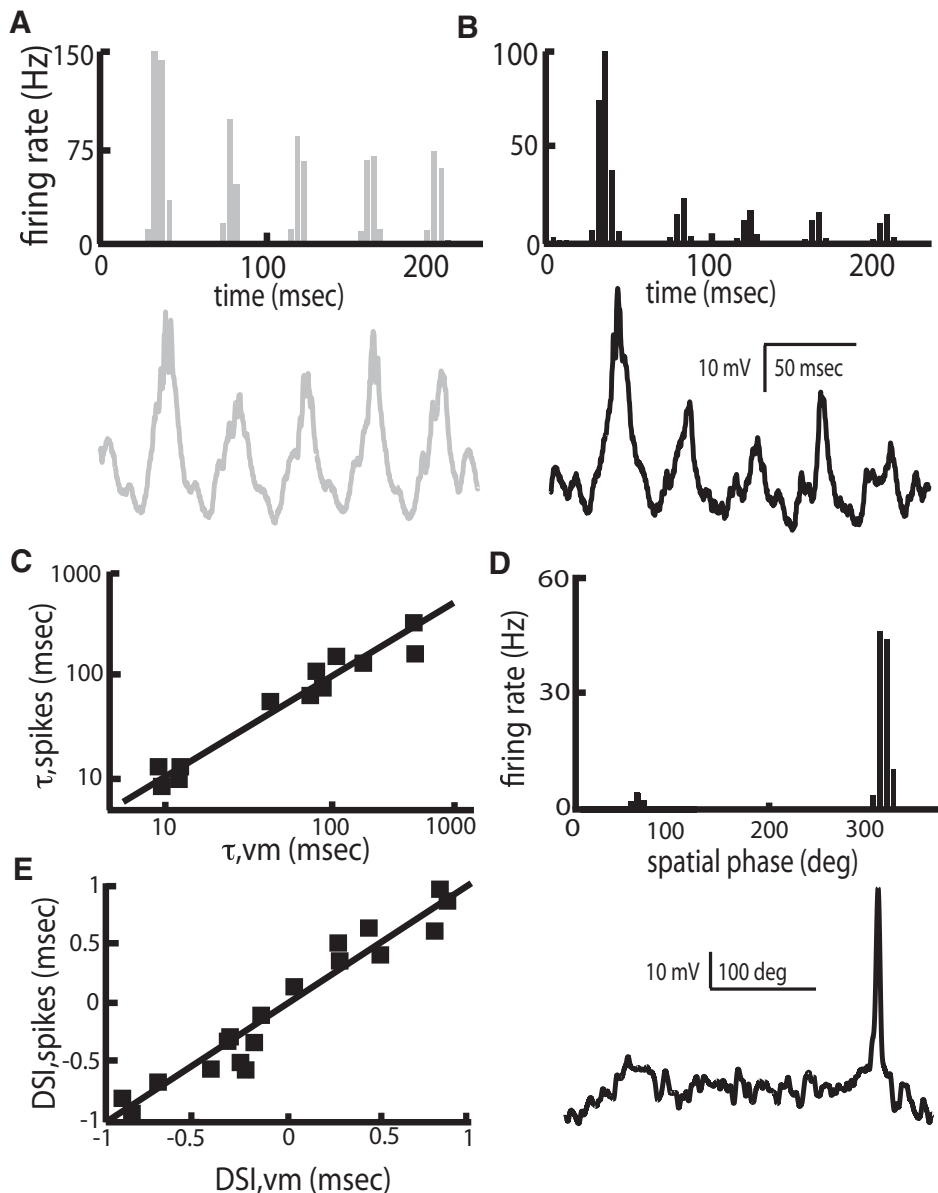


FIG. 8. TS neurons display similar characteristics in their spiking and membrane potential responses. *A*: comparison between the spiking (*top*) and subthreshold membrane potential (*bottom*) responses from a directionally selective TS neuron. It is seen that the depression in the spiking response is matched by a depression (i.e., a decrease in the PSP amplitude) in the subthreshold membrane potential. *B*: comparison between the spiking (*top*) and subthreshold membrane potential (*bottom*) responses from the same neuron when stimulated at a different location within the receptive field. The faster depression in the spiking response is matched by a faster depression of the PSP amplitude in the subthreshold membrane potential response. *C*: time constants of depression obtained from spiking responses and membrane potential responses to stationary stimuli at different spatial locations within the receptive field are strongly correlated ($R = 0.81$, $P < 10^{-3}$, $n = 13$) and equal in magnitude because most points are positioned on the identity line (solid line). This indicates that the depression of the spiking response is mediated by depression of the subthreshold membrane potential response. *D*: comparison of the spiking (*top*) and subthreshold (i.e., with spikes removed) membrane potential (*bottom*) responses of the same neuron to a moving object stimulus. It is seen that increases in firing rate are accompanied by strong membrane depolarizations and that both responses display similar directional biases. *E*: DSI values obtained from the spiking response were strongly correlated to the DSI values obtained from the subthreshold membrane potential response across our data sample ($R = 0.99$, $n = 18$, $P \ll 10^{-3}$). Moreover, all points were positioned across the identity line (solid line), indicating that the directional selectivity of the spiking response is equal in magnitude to the directional selectivity present in the subthreshold membrane potential response.

DISCUSSION

Summary of results

We investigated the directional responses of TS neurons in a species of weakly electric fish, *Apteronotus leptorhynchus*, to moving electrosensory objects. Most neurons in the TS were directionally selective, with a roughly equal distribution of neurons that preferred movement in the head-to-tail direction and tail-to-head directions. In contrast, neurons in the ELL, which are the sole source of ascending electrosensory information to TS neurons, did not exhibit directional selectivity. Therefore directional selectivity emerges at the level of the TS.

We first investigated whether differential steady-state filtering across the RF of TS neurons (e.g., center-surround) could account for their directionally biased responses. Although many TS neurons displayed center-surround organization that could theoretically underlie direction selectivity, just as many TS neurons with strong directional selectivity did not exhibit

center-surround RF organization. We built a simple mathematical model that incorporated the responses at different rostrocaudal positions and used it to predict the directional bias for each neuron in the study. We did not find any significant correlation between predicted and experimentally measured directional selectivity in relation to center-surround organization of RFs.

This led us to investigate whether differential filtering of transient stimuli across the RF could account for directional selectivity in TS neurons. We found that some TS neurons could display large variations in depression time constants to transient stimuli across their RFs. We then built a mathematical model incorporating the depression time constants measured at different rostrocaudal positions and used this model to predict the directional bias for a given neuron. We found a strong and significant correlation between the predicted and experimentally measured directional selectivity in relation to differences in short-term depression across the RF.

Intracellular recordings then revealed that depression in the spiking response was caused by depression of PSPs in the subthreshold membrane potential response. The directional bias of the subthreshold membrane potential was in fact equal to that of the spiking response. Finally, our data strongly argue against ELL pyramidal cell heterogeneities being the cause for directional selectivity in TS neurons.

Short-term depression as a mechanism for generating a directional bias

Previous modeling studies have shown that differential temporal filtering of input coming from different areas within the receptive field is sufficient to give rise to directionally biased response properties (Reichardt 1969). This differential temporal filtering could come from a multitude of mechanisms including, but not restricted to, delay lines (Reichardt 1969), differential excitation and inhibition, and short-term depression (Carver et al. 2008; Chance et al. 1998). Our results show experimentally, for the first time, that the differential temporal filtering created by short-term depression correlates with directional biases. The most likely source of differences in short-term depression is short-term synaptic depression: homosynaptic depression has been demonstrated to occur in ELL to TS synapses (Fortune and Rose 2000).

This conclusion is supported by the fact that differences in the ELL segments do not seem to contribute to directional selectivity in TS. Further, the depression time constants that we measured appear to form two clusters (Fig. 7C), suggesting that there may be two classes of ELL–TS neuron synapses: one group displays fast short-term depression on the approximately 10-ms timescale, whereas the other displays slower short-term depression on the roughly 100- to 300-ms timescale. Further studies preferably conducted *in vitro*, however, are necessary to test this hypothesis. In *Eigenmannia virescens*, short-term depression in TS neurons was typically best fit by a double exponential, with time constants on the order of tens of milliseconds and seconds (Fortune and Rose 2000). This is consistent with results obtained in cortical neurons (Varela et al. 1997). Further, a modeling study suggests that these two clusters of time constants could serve two functions—the shorter time constant mediating direction selectivity and the longer time constant mediating an enhancement of direction selectivity (Carver et al. 2008).

The evidence for the involvement of short-term synaptic depression in generating directional selectivity in TS neurons presented here is correlative—the phenomenon is understood only across the population of neurons in the study. In the best of cases, we would be able to manipulate short-term synaptic depression in a single recording and directly show an effect on direction selectivity. At present, however, this is not possible in the intact organism. Short-term synaptic depression at ELL–TS synapses is believed to be presynaptic (Fortune and Rose 2000) and thus it is currently impossible to block it with pharmacological agents. Further, because short-term synaptic depression is an activity-dependent process, any manipulation of the afferent activity that would affect short-term synaptic depression will also necessarily involve a change in the spatiotemporal pattern of action potentials arriving at the direction-selective neuron. This is problematic because the direction-selective computation is performed on the spatiotemporal

pattern of activity arriving at the TS neuron. Nevertheless, our correlative evidence involves several methods of analysis (i.e., the greatest difference in time constants across the RF, X–T plots, and a mathematical model incorporating the experimentally measured depression time constants) and matches previous predictions from modeling studies (Carver et al. 2008; Chance et al. 1998).

Comparing the mechanisms of directional selectivity across species

Differences in temporal filtering of input coming from different zones within the RF lead to directionally biased responses (Reichardt 1969). It is therefore not surprising that the mechanisms that mediate directional selectivity to movement are quite diverse and vary across sensory modalities and species. In fact, these can take the form of different low-pass filters, as observed in the insect visual system (Borst 2007; Borst and Egelhaaf 1989), different dendritic integration in rabbit retinal ganglion cells (Taylor et al. 2000; Yang and Masland 1992), and differential delays in mammalian visual cortex (Jagadeesh et al. 1993, 1997). These mechanisms could be used in other spatiotemporal computations. For example, selectivity to ascending or descending frequency-modulated acoustic sweeps has been observed in mammalian inferior colliculus (IC) and auditory cortex (Fuzessery and Hall 1996; Fuzessery et al. 2006; Razak and Fuzessery 2006, 2008; Suga 1965). In particular, it has been shown that three mechanisms—facilitation, sideband inhibition, and duration tuning—mediate directional selectivity in the auditory system. Because TS and IC are homologous structures, comparisons between directional selectivity to movement in TS and directional selectivity to frequency sweeps in IC are particularly interesting. Previous studies have shown the presence of facilitation in ELL–TS synapses (Fortune and Rose 2000), although further studies are needed to ascertain its potential role in directional selectivity in TS.

Conclusion

We have provided the first experimental demonstration that differential time constants of short-term depression across the receptive field are correlated with responses to a moving stimulus. This mechanism is ubiquitous in vertebrate neural circuits (Boudreau and Ferster 2005) and may thus contribute to directional selectivity and other spatiotemporal computations across sensory modalities and species.

ACKNOWLEDGMENTS

We thank G. Pollack, K. Cullen, R. Krahe, S. Musallam, C. Pack, J. Martinez-Trujillo, S. Carver, and N. Cowan for useful discussions and critical readings of the manuscript; N. Hashemi for help with data analysis; and B. Dirlikov for experimental support.

GRANTS

This research was supported by National Science Foundation Grant 0543985 to E. S. Fortune; a Grass Foundation grant to E. S. Fortune and M. J. Chacron; and Canadian Institutes of Health Research, Natural Sciences and Engineering Research Council of Canada, Canada Foundation for Innovation, and Canada Research Chairs grants to M. J. Chacron.

REFERENCES

Adelson EH, Bergen JR. Spatiotemporal energy models for the perception of motion. *J Opt Soc Am A Opt Image Sci Vis* 2: 284–299, 1985.

- Bastian J.** Electrolocation. II. The effects of moving objects and other electrical stimuli on the activities of two categories of posterior lateral line lobe cells in *Apteronotus albifrons*. *J Comp Physiol A Sens Neural Behav Physiol* 144: 481–494, 1981.
- Bastian J, Chacron MJ, Maler L.** Receptive field organization determines pyramidal cell stimulus-encoding capability and spatial stimulus selectivity. *J Neurosci* 22: 4577–4590, 2002.
- Borst A.** Correlation versus gradient type motion detectors: the pros and cons. *Philos Trans R Soc Lond B Biol Sci* 362: 369–374, 2007.
- Borst A, Egelhaaf M.** Principles of visual motion detection. *Trends Neurosci* 12: 297–306, 1989.
- Boudreau CE, Ferster D.** Short-term depression in thalamocortical synapses of cat primary visual cortex. *J Neurosci* 25: 7179–7190, 2005.
- Carr CE, Maler L.** A Golgi study of the cell types of the dorsal torus semicircularis of the electric fish *Eigenmannia*: functional and morphological diversity in the midbrain. *J Comp Neurol* 235: 207–240, 1985.
- Carver S, Roth E, Cowan NJ, Fortune ES.** Synaptic plasticity can produce and enhance direction selectivity. *PLoS Comput Biol* 4: e32, 2008.
- Chacron MJ.** Nonlinear information processing in a model sensory system. *J Neurophysiol* 95: 2933–2946, 2006.
- Chacron MJ, Bastian J.** Population coding by electrosensory neurons. *J Neurophysiol* 99: 1825–1835, 2008.
- Chacron MJ, Doiron B, Maler L, Longtin A, Bastian J.** Non-classical receptive field mediates switch in a sensory neuron's frequency tuning. *Nature* 423: 77–81, 2003.
- Chacron MJ, Maler L, Bastian J.** Feedback and feedforward control of frequency tuning to naturalistic stimuli. *J Neurosci* 25: 5521–5532, 2005.
- Chance FS, Nelson SB, Abbott LF.** Synaptic depression and the temporal response characteristics of V1 cells. *J Neurosci* 18: 4785–4799, 1998.
- Cowan NJ, Fortune ES.** The critical role of locomotion mechanics in decoding sensory systems. *J Neurosci* 27: 1123–1128, 2007.
- Fortune ES.** The decoding of electrosensory systems. *Curr Opin Neurobiol* 16: 474–480, 2006.
- Fortune ES, Rose GJ.** Short-term synaptic plasticity contributes to the temporal filtering of electrosensory information. *J Neurosci* 20: 7122–7130, 2000.
- Frank K, Becker MC.** Microelectrodes for recording and stimulation. In: *Physical Techniques in Biological Research, Part A*. New York: Academic, 1964, p. 23–84.
- Fuzessery ZM, Hall JC.** Role of GABA in shaping frequency tuning and creating FM sweep selectivity in the inferior colliculus. *J Neurophysiol* 76: 1059–1073, 1996.
- Fuzessery ZM, Richardson MD, Coburn MS.** Neural mechanisms underlying selectivity for the rate and direction of frequency-modulated sweeps in the inferior colliculus of the pallid bat. *J Neurophysiol* 96: 1320–1336, 2006.
- Heiligenberg W.** *Neural Nets in Electric Fish*. Cambridge, MA: MIT Press, 1991.
- Hitschfeld ÉM, Stamper SA, Vonderschen K, Fortune ES, Chacron MJ.** Effects of restraint and immobilization on electrosensory behaviors of weakly electric fish. *ILAR Journal* 50: 361–372, 2009.
- Hubel D.** Single unit activity in striate cortex of unrestrained cats. *J Physiol* 147: 226–238, 1959.
- Hubel DH, Wiesel TN.** Receptive fields, binocular interaction and functional architecture in the cat's visual cortex. *J Physiol* 160: 106–154, 1962.
- Jagadeesh B, Wheat HS, Ferster D.** Linearity of summation of synaptic potentials underlying direction selectivity in simple cells of the cat visual cortex. *Science* 262: 1901–1904, 1993.
- Jagadeesh B, Wheat HS, Kontsevich LL, Tyler CW, Ferster D.** Direction selectivity of synaptic potentials in simple cells of the cat visual cortex. *J Neurophysiol* 78: 2772–2789, 1997.
- Krahe R, Bastian J, Chacron MJ.** Temporal processing across multiple topographic maps in the electrosensory system. *J Neurophysiol* 100: 852–867, 2008.
- MacIver MA, Sharabash NM, Nelson ME.** Prey-capture behavior in gymnotid electric fish: motion analysis and effects of water conductivity. *J Exp Biol* 204: 543–557, 2001.
- Maler L.** The posterior lateral line lobe of certain gymnotiform fish. Quantitative light microscopy. *J Comp Neurol* 183: 323–363, 1979.
- Maler L, Sas E, Johnston S, Ellis W.** An atlas of the brain of the weakly electric fish *Apteronotus leptorhynchus*. *J Chem Neuroanat* 4: 1–38, 1991.
- Maler L, Sas EK, Rogers J.** The cytology of the posterior lateral line lobe of high frequency weakly electric fish (*Gymnotoidei*): differentiation and synaptic specificity in a simple cortex. *J Comp Neurol* 195: 87–139, 1981.
- Nelson ME, MacIver MA.** Prey capture in the weakly electric fish *Apteronotus albifrons*: sensory acquisition strategies and electrosensory consequences. *J Exp Biol* 202: 1195–1203, 1999.
- Newbold P.** *Statistics for Business and Economics*. Englewood Cliffs, NJ: Prentice Hall, 2006, p. 984.
- Priebe NJ, Ferster D.** Direction selectivity of excitation and inhibition in simple cells of the cat primary visual cortex. *Neuron* 45: 133–145, 2005.
- Priebe NJ, Ferster D.** Inhibition, spike threshold, and stimulus selectivity in primary visual cortex. *Neuron* 57: 482–497, 2008.
- Ramcharitar JU, Tan EW, Fortune ES.** Effects of global electrosensory signals on motion processing in the midbrain of *Eigenmannia*. *J Comp Physiol A Sens Neural Behav Physiol* 191: 865–872, 2005.
- Ramcharitar JU, Tan EW, Fortune ES.** Global electrosensory oscillations enhance directional responses of midbrain neurons in *Eigenmannia*. *J Neurophysiol* 96: 2319–2326, 2006.
- Razak KA, Fuzessery ZM.** Neural mechanisms underlying selectivity for the rate and direction of frequency-modulated sweeps in the auditory cortex of the pallid bat. *J Neurophysiol* 96: 1303–1319, 2006.
- Razak KA, Fuzessery ZM.** Facilitatory mechanisms underlying selectivity for the direction and rate of frequency modulated sweeps in the auditory cortex. *J Neurosci* 28: 9806–9816, 2008.
- Reichardt W.** Editor. *Movement Perception in Insects*. New York: Academic Press, 1969.
- Reichardt W.** Evaluation of optical motion information by movement detectors. *J Comp Physiol A Sens Neural Behav Physiol* 161: 533–547, 1987.
- Rose GJ, Fortune ES.** New techniques for making whole-cell recordings from CNS neurons *in vivo*. *Neurosci Res* 26: 89–94, 1996.
- Rose GJ, Fortune ES.** Frequency-dependent PSP depression contributes to low-pass temporal filtering in *Eigenmannia*. *J Neurosci* 19: 7629–7639, 1999.
- Shumway C.** Multiple electrosensory maps in the medulla of weakly electric Gymnotiform fish. I. Physiological differences. *J Neurosci* 9: 4388–4399, 1989a.
- Shumway C.** Multiple electrosensory maps in the medulla of weakly electric Gymnotiform fish. II. Anatomical differences. *J Neurosci* 9: 4400–4415, 1989b.
- Sillito AM, Kemp JA, Blakemore C.** The role of GABAergic inhibition in the cortical effects of monocular deprivation. *Nature* 291: 318–320, 1981.
- Suga N.** Responses of cortical auditory neurones to frequency modulated sounds in echo-locating bats. *Nature* 206: 890–891, 1965.
- Taylor WR, He S, Levick WR, Vaney DI.** Dendritic computation of direction selectivity by retinal ganglion cells. *Science* 289: 2347–2350, 2000.
- Toporikova N, Chacron MJ.** Dendritic SK channels gate information processing *in vivo* by regulating an intrinsic bursting mechanism seen *in vitro*. *J Neurophysiol* (August 12, 2009). doi:10.1152/jn.00282.2009.
- Turner RW, Maler L, Burrows M.** Electroreception and electrocommunication. *J Exp Biol* 202: 1167–1458, 1999.
- Varela JA, Sen K, Gibson J, Frost J, Abbott LF, Nelson SB.** A quantitative description of short-term plasticity at excitatory synapses in layer 2/3 of rat primary visual cortex. *J Neurosci* 17: 7926–7940, 1997.
- Yang G, Masland RH.** Direct visualization of the dendritic and receptive fields of directionally selective retinal ganglion cells. *Science* 258: 1949–1952, 1992.